EXTENSION OF PRESTON'S SHEAR MEASUREMENT TECHNIQUE TO ROUGH BOUNDARIES

Thesis for the Degree of M. S.
MICHIGAN STATE UNIVERSITY

Li-San Hwang

1962

This is to certify that the

thesis entitled

"Extension of Preston's Shear Measurement Technique to Rough Boundaries"

presented by

Li-San Hwang

has been accepted towards fulfillment of the requirements for

M.S. degree in Civil Engineering

Major professor

Date February 23, 1962

O-169

EXTENSION OF PRESTON'S SHEAR MEASUREMENT TECHNIQUE TO ROUGH BOUNDARIES

By

Li-San Hwang

A THESIS

Submitted to
Michigan State University
in partial fulfillment of the requirements
for the degree of

MASTER OF SCIENCE

Department of Civil Engineering

1962

ACKNOWLEDGEMENTS

The author is indebted to Dr. E. M. Laursen, without whose guidance and encouragement, this thesis would not have been possible; he also wishes to express his gratitude to Dr. H. R. Henry for his review of the manuscript, to Dr. C. P. Wells for his review of the analytical result, and to his colleague, Mr. J. R. Adams for his assistance. The research upon which this thesis is based was part of a larger study on "Pressure and Shear Distribution on Dune-shaped Boundaries," conducted under a grant from the National Science Foundation.

TABLE OF CONTENTS

		Page
NOTATION		iv
I.	INTRODUCTION	1
II.	ANALYSIS	4
III.	EXPERIMENTS	10
IV.	RESULTS AND DISCUSSION	13
V.	CONCLUSIONS	17
BIBLIOGRAPHY		27

NOTATION

A	$30\ h/k_s$
a	Inner radius of the stagnation tube
B	$30\ a/k_s$
b	Outer radius of the stagnation tube
C	Coefficient in Kármán-Prandtl velocity equation
D	Coefficient in Kármán-Prandtl velocity equation
f	Resistance coefficient
h	Height of center of stagnation tube from zero datum
k_s	Sand roughness
m	Dummy integration parameter
P	Stagnation pressure
P_o	Wall static pressure
R	Reynolds number
r_o	Inner radius of the tubing
u	Velocity at distance y from wall
$u*$	Shear velocity = $\sqrt{\tau_o/\rho}$
y	Distance from zero datum
z_o	Height of bottom of stagnation tube from zero datum
Γ	Gamma function
δ'	Thickness of laminar sublayer
θ	Integration parameter

ν Kinematic viscosity

ρ Density of fluid

σ Area of stagnation tube opening

τ_o Wall shear stress

$\left(\frac{P-P_o}{\tau_o}\right)_a$ Analytical pressure-shear ratio, in completely rough regime

$\left(\frac{P-P_o}{\tau_o}\right)_e$ Experimental pressure-shear ratio, in completely rough regime

ABSTRACT

EXTENSION OF PRESTON'S SHEAR MEASUREMENT TECHNIQUE TO ROUGH BOUNDARIES

by Li-San Hwang

Preston's shear measurement technique consists of placing a pitot tube in contact with a wall and interpreting the dynamic pressure reading obtained as a measure of the local shear on the wall. The rationale of the technique is that the velocity distribution near the wall is a function only of conditions at the wall, and the dynamic pressure reading in the tube is determined by the velocity distribution and the tube size. Assuming the Kármán-Prandtl velocity distribution, an analysis was performed for the fully rough flow regime which gives the ratio of the dynamic pressure reading to the wall shear as a function of the tube size and of the roughness element. Experimental measurements provided correction factors for the particular roughness used and for the transition regime of flow. Satisfactory results were obtained indicating that Preston's technique can be used for rough boundaries.

I. INTRODUCTION

Detailed knowledge of the local boundary shear is needed in many problems of fluid mechanics. Since analysis can seldom provide the desired answer if the flow is turbulent, one must resort to experimental measurement techniques. The empirical data from measurements may be immediately helpful in practical problems, or may be useful in the building of theory.

Direct measurement of boundary shear has been attempted, but has not been entirely successful. To obtain a direct measurement of the shear on the boundary, one must measure the shear force on a small isolated floating element of the surface.[1] Maintaining a small gap around the floating element, keeping it in the correct position, and recording the small shear force acting on the element are all difficult problems. An inherent disadvantage to this type of instrument is that it is restricted to a predetermined fixed point, thus inhibiting the free exploration of the shear distribution on the boundary surfaces.

A standard indirect technique in boundary layer studies has been the measurement of the velocity and pressure profile normal to the boundary at successive sections and solving for the shear by the momentum principle.[2] If the shear is small or varies in a manner which is not simple, the results are less satisfactory, since the shear is obtained as the small difference between large values.

Ludweig developed an indirect method which relates shear force to the heat loss from a hot-spot on the boundary to the flow medium.[3] The insulation between the hot-spot and its surroundings must be excellent or considerable error may result. This method is not adapted to the evaluation of unknown shear distributions as it is restricted to measurements at pre-chosen fixed points. Moreover, the method can only be used when there is a laminar sublayer.

In 1954 J. A. Preston successfully developed a simple technique for measuring the local shear on smooth boundaries using a pitot tube in contact with the surfaces.[4] This method is based upon the assumption of an inner law relating the local shear to the velocity distribution near the wall. Using the pressure drop in a pipe to calibrate the instrument, Preston obtained equations relating the shear to the pitot tube reading both for the case of the laminar sublayer enveloping the tube, and for the case of the tube in the turbulent boundary layer on the smooth surface.

E. Y. Hsu used the velocity distribution equations, $u/u^* = k\, y^{1/7}$ (turbulent boundary layer) and $u/u^* = u^*\, y/\nu$ (laminar sublayer), to establish analytical relationships between the dynamic pressure reading and the local boundary shear.[5] Hsu's analysis agrees well with Preston's experimental results and also appears to give good results for the boundary layer on a flat plate with ambient pressure gradients. In the present investigation an experiment was performed with a pipe to check equipment and technique. The results agreed, as expected, with Preston's and Hsu's.

In practice the boundaries of the flow are more likely to be rough than smooth. Thus, an extension of Preston's relatively simple technique to rough boundaries would be very useful. An analytical relationship has been developed between the dynamic pressures acting on the pitot tube in contact with the rough surface and the local boundary shear. The relation is a function of the inside diameter of the tube, the size of the roughness, and the position of the tube in relation to the zero datum for flow in the completely rough regime. For the transition and hydraulically smooth regimes one more parameter, the ratio of the roughness to the laminar sublayer is needed. The effect of this parameter has been assessed experimentally.

II. ANALYSIS

The concept of the inner law is that the velocity distribution near a rough boundary depends only upon the viscosity and the density of the fluid, the roughness of the boundary, and the shear stress at the wall. The Kármán-Prandtl velocity distribution equation which is generally considered to be a satisfactory approximation for pipes and channels and is often used in other situations, can be expressed as follows

$$u/u_* = C \log y/k_s + D \quad \ldots\ldots\ldots\ldots\ldots\ldots \quad (1)$$

The classic systematic experiments of J. Nikuradse utilized pipes covered tightly on the inside with ordinary building sand.[6] For better adherence of the sand grains, the pipe was filled and emptied a second time with Japanese lacquer after the inside had been coated with sand grains. The values usually quoted for C and D are based on Nikuradse's data, $C = 5.75$ and $D = 8.5$, except in the transition regime where D is a function of $u_* k_s/\nu$ or k_s/δ'. Although the adequacy of this logarithmic equation can be debated, especially near the boundary, and the indeterminancy of the zero datum presents difficulties, Eq. (1) has been adopted for this analysis. Further assumptions which have been used in the analysis are:

(1) The disturbance of the flow caused by the presence of the tube on the rough boundary may be neglected.

(2) The dynamic pressure acting on surface pitot tube, and therefore the reading obtained, is the average of $\rho u^2/2$ over the open area.

With the above assumptions, the dynamic pressure acting on the tube, as shown in Fig. 1, can be correlated to the local boundary shear by

$$(P-P_o)\pi a^2 = \frac{1}{2}\rho \int_\sigma u^2 \, d\sigma \quad \ldots\ldots\ldots\ldots \quad (2)$$

or

$$\frac{P-P_o}{\tau_o} = \frac{1}{2\pi a^2} \int_\sigma \left(\frac{u}{u_*}\right)^2 d\sigma$$

In the completely rough regime, i.e., where $u_* k_s/\nu > 70$, Eq. (1) can be written in the form

$$u/u_* = 5.75 \log 30\, y/k_s \quad \ldots\ldots\ldots\ldots\ldots \quad (3)$$

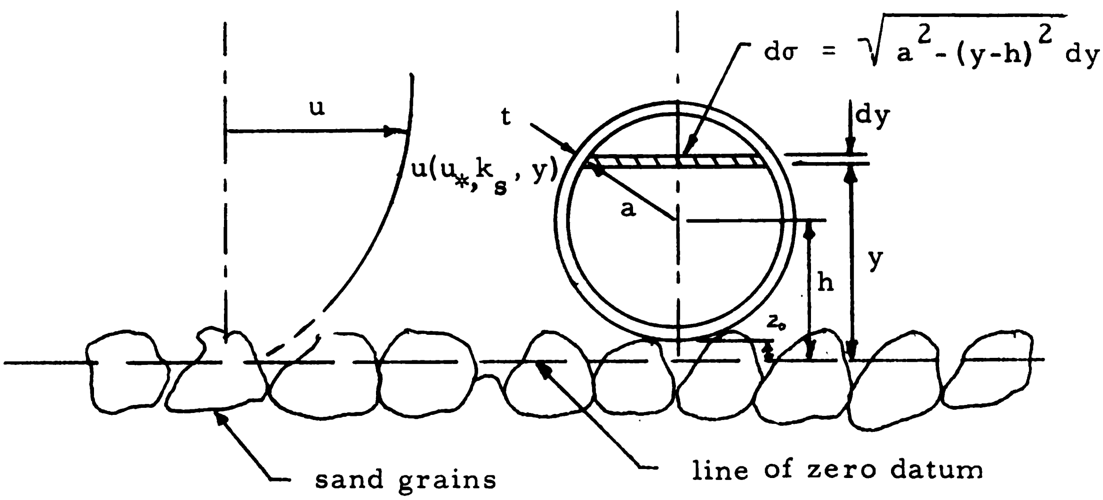

Fig. 1. A stagnation tube resting on a rough boundary

Substituting Eq. (3) into Eq. (2) results in

$$\frac{P-P_o}{\pi a^2} \doteq \frac{1}{2} \int_{h-a}^{h+a} [5.75\, u_* \log \frac{30\, y}{k_s}]^2 \cdot 2 \cdot \sqrt{a^2-(y-h)^2}\, dy \quad (4)$$

This integral relation can be evaluated in the following way: Let

$y = h + a \sin\theta$,

$A = 30\, h/k_s$,

$B = 30\, a/k_s \cdot$ (where $A > B$)

Making these substitutions in Eq. (4), and changing integration limits, one obtains,

$$\frac{P-P_o}{\tau_o} = \frac{(5.75)^2}{\pi} \int_{-\frac{\pi}{2}}^{\frac{\pi}{2}} [\log(A+B\sin\theta]^2 \cos^2\theta\, d\theta$$

$$= \frac{(5.75)^2}{2\pi} \int_{o}^{2\pi} [\log(A+B\sin\theta)]^2 \cos^2\theta\, d\theta \quad \ldots\ldots \quad (5)$$

Now let $f(m) = A^m \int_{o}^{2\pi} (1+\frac{B}{A}\sin\theta)^m \cos^2\theta\, d\theta \quad \ldots\ldots\ldots\ldots \quad (6)$

Upon expanding the integrand, there is obtained,

$$f(m) = A^m \int_{o}^{2\pi} (1+m\frac{B}{A}\sin\theta + (\frac{m}{2})\frac{B^2}{A^2}\sin^2\theta + (\frac{m}{3})\frac{B^3}{A^3}\sin^3\theta + \ldots)\cos^2\theta\, d\theta$$

The odd powers of $\sin\theta$ disappear and the even powers can be integrated through the relation between the gamma and trigonometric functions,[7]

$$\int_0^{\frac{\pi}{2}} \cos^{s-1} x \sin^{n-1} x \, dx = \frac{1}{2} \frac{\Gamma(\frac{1}{2}s)\,\Gamma(\frac{1}{2}n)}{\Gamma(\frac{1}{2}s + \frac{1}{2}n)}$$

then

$$f(m) = 4A^m\left[\frac{\pi}{4} + \binom{m}{2}\frac{B^2}{A^2}\frac{1}{2}\frac{\Gamma(\frac{3}{2})\,\Gamma(\frac{3}{2})}{\Gamma(3)} + \binom{m}{4}\frac{B^4}{A^4}\frac{1}{2}\frac{\Gamma(\frac{5}{2})\,\Gamma(\frac{3}{2})}{\Gamma(4)} + \ldots\right]$$

The gamma functions can be evaluated by the relation

$$\Gamma(s+1) = s\,\Gamma(s),$$

and $\Gamma(1) = 1$ and $\Gamma(\frac{1}{2}) = \sqrt{\pi}$.

Then

$$f(m) = 2\pi A^m\left[\frac{1}{2} + \binom{m}{2}\frac{B^2}{A^2}\frac{1}{2\cdot 4} + \binom{m}{4}\frac{1\cdot 3\cdot 1}{2\cdot 4\cdot 6}\frac{A^4}{B^4}\cdot\cdot\cdot\right] \qquad (7)$$

Let $\phi(m) = \frac{1}{2} + \binom{m}{2}\frac{1}{2\cdot 4}\frac{B^2}{A^2} + \binom{m}{4}\frac{1\cdot 3\cdot 1}{2\cdot 4\cdot 6}\frac{B^4}{A^4} + \ldots.$

Then

$$f(m) = 2\pi A^m \phi(m) \quad \ldots\ldots\ldots\ldots\ldots\ldots\ldots \quad (8)$$

Differentiating Eqs. (6) and (8) with respect to m twice and putting $m = 0$, one obtains

$$f''(0) = \int_0^{2\pi} [\log(A + B\sin\theta)]^2 \cos^2\theta \, d\theta$$

$$= 2\pi \log^2 A\,\phi(0) + 4\pi \log A\,\phi'(0) + 2\pi\phi''(0) \quad \ldots\ldots\ldots\ldots \quad (9)$$

Substituting Eq. (9) and the values of A and B into Eq. (5) there results

$$\frac{P-P_o}{\tau_o} = 16.531 \left\{ \left[\log \frac{30\,h}{k_s} \right]^2 - \log \frac{30\,h}{k_s} \left[0.25 \left(\frac{a}{h}\right)^2 + 0.0833 \left(\frac{a}{h}\right)^4 + 0.0704 \left(\frac{a}{h}\right)^6 + \ldots \right] + \left[0.25 \left(\frac{a}{h}\right)^2 + 0.1146 \left(\frac{a}{h}\right)^4 + 0.0586 \left(\frac{a}{h}\right)^6 + \ldots \right] \right\} \qquad \ldots. \ (10)$$

This series converges quite rapidly, especially when the ratio a to h is small.

Given an inside tube diameter and a roughness size a/k_s, the pressure-shear ratio $(P-P_o)/\tau_o$, varies with the relative position of the tube as shown in Fig. 4. The relative position of the tube $(h - a)/k_s$ can also be written as $z_o/k_s + t/k_s$, where z_o is the distance from the zero datum to the outside bottom of the tube and t is the thickness of the tube wall. If the tube is large compared to the sand particle, z_o equals the distance from the datum to the top of the particles, or something less than $0.5\ k_s$. If the tube is small it may rest below the top of the particles but z_o/k_s would probably be greater than zero. Intuitively, one might estimate that z_o/k_s would fall between 0.1 and 0.4.

Examination of Fig. 4 shows that the larger the tube opening, the greater the pressure-shear ratio and the less the effect of unknowable z_o/k_s values. Therefore, the tube should be chosen as large as possible, but within the region in which the velocity distribution is primarily determined by the boundary shear and in which the general overall boundary configuration has little influence.

The above analysis assumes that the flow is in the completely rough regime. In the hydraulically smooth and transitional regimes, D is no longer constant, but a function of $u_* k_s/\nu$. The pressure-shear ratio then would be a function of three parameters a/k_s, $(h-a)/k_s$, and $u_* k_s/\nu$.

Given values of C and D for various values of $u_* k_s/\nu$ one could obtain relationships similar to Eq. (10), or a correction factor. Because the values of C and D are open to question (in fact the applicability of the logarithmic velocity distribution itself so close to the boundary is debatable), this analysis has not been performed. Instead, the correction factor is presented as an empirical formulation based on the experimental data.

III. EXPERIMENTS

The general arrangement of the apparatus is shown in Fig. 2. The tubing consisted of four sections each 10 ft. in length, of 6-in. outside diameter and 1/8-in. wall thickness. These were split lengthwise for access when covering the interior surface of the tube with sandpaper. A pair of steel bars, welded on each side of the tubing before splitting, were used to bolt the split tubing together. The width of the saw cuts was compensated for by gaskets which maintained the circular cross-section and formed air-tight seals.

Two pairs of peizometers were used on each of the first three sections of the tubing. In each section, the first pair of peizometers is located 4 ft. downstream from the joint and the other pair 1 ft. upstream from the next joint.

Five series of tests were performed: one with the comparatively smooth surface of the steel pipe and others with rough surfaces of four different grades of sandpaper. The sandpaper, with grit numbers 36, 80, 150 and 220 corresponding to nominal grain sizes of 0. 75, 0. 35, 0. 17 and 0. 06 mm. respectively, was obtained from the Minnesota Mining and Manufacturing Company. The grades were chosen for a ratio of approximately 1/2 between the different grades. All were of the open-coat type of production paper with sharp grains. Microphotographs of the sandpapers are shown in Fig. 5. The sandpaper was glued to the tubing with "Feathering Disc Adhesive," also a product of the 3M Company.

For the smooth boundary case, the peizometers were 1/16-in. diameter holes drilled through the tubing with 1/4-in. diameter and 3/4-in. long nipples soldered to the outside of the tubing. For the rough boundary cases, the design of the peizometers is shown in Fig. 2c. The smooth plate of 1-in. diameter and 0.008-in. thick brass was used to avoid the possibility of the wakes from discrete sand particles influencing the pressure measurements. The set screw was used to orient the curved plate along the tube axis, and to permit adjustment of the height of the plate for the various sandpapers. The peizometer was connected to an alcohol manometer, which had a direct vernier reading of 1/1000 ft. Fig. 6 is a typical plot of pressure drop along the tubing. The measurements lie nearly on a straight line. Each pair of peizometers gave consistent results, with only slight differences between the top and bottom taps.

The dynamic pressure was obtained by subtracting the static pressure from the total pressure measured by a stagnation tube. The several stagnation tubes used were made from hypodermic needles with the inside diameters and the ratios of inside to outside diameter given in Table I. The measurement of the total pressures was taken 1.5 in. from the exit. To aid in precise positioning of the tube on the rough boundary, a lamp was placed so that the light visible

Table I

Stagnation tube number	1	2	3	4
Internal dia. 10^{-2} in.	8.55	6.25	4.65	3.10
Ratio I. D. / O. D.	0.78	0.75	0.72	0.64

between the stagnation tube and the boundary could be observed, and the stagnation tube adjusted to equalize the amount of light visible along the length of the tube. The static pressure was measured by a static tube which had the same diameter as stagnation tube number 3, with four small holes of 0.020 in. in diameter, located eight outside diameters from the tip of the hemispherical nose.

For each run the total pressure was measured by recording values at eight positions around the periphery of the tubing except in the vicinity of the junction of the two halves of the tubing. The average of these eight readings was used in the calculations.

IV. RESULTS AND DISCUSSION

The experimental results for all four tubes on the smooth steel surface are plotted in Fig. 3. They agree with Preston's experimental results very well. Preston's empirical and Hsu's analytical equations are plotted in the figure. On the basis of this agreement it was assumed that the equipment and techniques used in this investigation were satisfactory and could also be used on rough boundaries.

The dynamic pressure readings taken with the stagnation tube resting on the sand-roughened boundary are quite consistent. However, the readings taken at the eight peripheral positions were not exactly alike. The differences can probably be attributed to the variation in the roughness texture and, therefore, the position of the tube relative to the zero datum. A variation in the velocity distribution is also possible, but would be small and have less influence. The possible positioning errors in the pressure readings with the different sand roughnesses and different stagnation tubes are shown in Table II. The errors are expressed in percent error at a 0.90 degree level of confidence using the t-test.[8] The table shows that the error increases as sand roughness increases and decreases as the size of the tube increases. The larger, and erratic, errors of the low velocity runs reflect the effect of the least reading of the manometer. Although an individual reading may be several percent in error, the average should be reasonably accurate.

Table II. Typical Error in % in Pressure Reading

Sandpaper no.	36		80		150		220	
Velocity	H	L	H	L	H	L	H	L
Tube no.								
1	±2.6	±2.8	±1.5	±4.9	±0.9	±2.9	±1.6	±2.9
2	±2.1	±3.2	±1.7	±4.0	±0.9	±2.1	±1.8	±3.0
3	±3.3	±4.2	±2.4	±2.7	±1.3	±1.6	±1.0	±4.7
4	±4.5	±5.9	±2.1	±5.3	±1.0	±6.4	±1.8	±4.4

H: Highest velocity; L: Lowest velocity

Figure 7 shows that the value of f is somewhat larger than the value obtained by Nikuradse for the same roughness k_s. The following reasons might serve to explain this:

(a) The nominal size of the particles on the sandpaper may not be equivalent to Nikuradse's.

(b) The sandpaper used in this testing is of an open coat type, i.e. there is no glue or adhesive covering the sand grains. The effective roughness may be larger than that of a closed coat as used in Nikuradse's test.

(c) There are spaces between the particles on the sandpaper, whereas the description of Nikuradse's roughness would indicate the particles were quite tightly packed.[6]

(d) The sand used in this investigation is a crushed product of aluminum oxide having sharper corners and more irregular shapes than ordinary sand.

In Fig. 8, the ratio of the pressure to the shear as measured is compared to the pressure-shear ratio obtained analytically for fully rough flow as a function of the particle shear-velocity Reynolds number. The plot of

$$\frac{P-P_o}{\tau_o} / \left(\frac{P-P_o}{\tau_o}\right)_a$$

against log $u_* k_s/\nu$ is the familiar Nikuradse harp and represents the effect of a systematic variation in the velocity distribution in the transition region. The analytical pressure-shear ratio is obtained from Fig. 4 knowing a, k_s, and t and assuming $z_o/k_s = 0.15$, 0.20, 0.25 and 0.30 for sandpaper 36, 80, 150 and 220 respectively. Only for the roughest sandpaper does the z_o/k_s value present a problem. For the thinnest walled tube with the No. 80 sandpaper the pressure-shear ratio would only change 10% for extreme values of z_o/k_s of 0.1 and 0.5. The experimental data appear to be about 12% below the analytic line for the fully rough flow. Perhaps the reasons mentioned for the discrepancy in f values could also explain this discrepancy. Another reason could be the assumption of the velocity distribution since the pressure-shear ratio is quite sensitive to the velocity profile. J. M. Robertson analyzed Nikuradse's data and suggested the Kármán-

Prandtl velocity distribution should be written as $u/u_* = 5.6 \log y/k_s + 8.3$[9] instead of $u/u_* = 5.75 \log y/k_s + 8.5$. If Robertson's values of C and D are used in the analysis, the discrepancy between measurement and analysis would be reduced from 12% to 7%. The data from the experiments with the roughest sandpaper are plotted as

$$\frac{P-P_o}{\tau_o} / \left(\frac{P-P_o}{\tau_o}\right)_e$$

against $\log u_* k_s/\nu$ in Fig. 9, where the denominator is the experimental pressure shear ratio in the rough region. For this series of measurements the tubes were kept in a fixed position and the rate of flow varied. This could only be done for the experiments with the roughest sandpaper, for with the other sandpapers the data did not extend into the fully rough regime. This curve shows that the data obtained with the different sizes of stagnation tubes do not show any systematic scatter.

V. CONCLUSIONS

Although certain difficulties remain, it would appear that Preston's shear measurement technique can be used with rough boundaries. The difficulties are due to our inadequate knowledge of flow near rough boundaries, and may be simply stated as questions of what is the correct form of the velocity distribution and where is the zero datum.

The analysis which has been carried out using the commonly used Kármán-Prandtl velocity distribution provides a relationship which should give excellent qualitative values of shear, especially when used in conjunction with the empirical correction values for flow in the transition range. It would have been possible to achieve an excellent correlation between analysis and experiment by assuming other values for the coefficients C and D in the logarithmic velocity distribution (or other forms of the velocity distribution equation). This was not done because it would merely disguise the practical difficulty, which should be explicitly faced by anyone using this technique for measuring local shear; what is the "roughness" of any particular surface, and what is the velocity distribution near this particular surface?

For many problems a qualitative, or relative, measure of the local shear should be sufficient. For example, if one were to measure the distribution of shear in uniform flow in a trapezoidal channel, qualitative values could be corrected to agree with the total shear obtained from slope measurements. For such problems the pressure-shear ratio relations for fully rough flow presented in Fig. 4 and the correction factors presented in Fig. 8, should be directly applicable.

For problems in which a quantitative measure of shear is required, experiments such as performed in this investigation would permit the development of correction factors similar to Fig. 8 for the particular roughness involved.

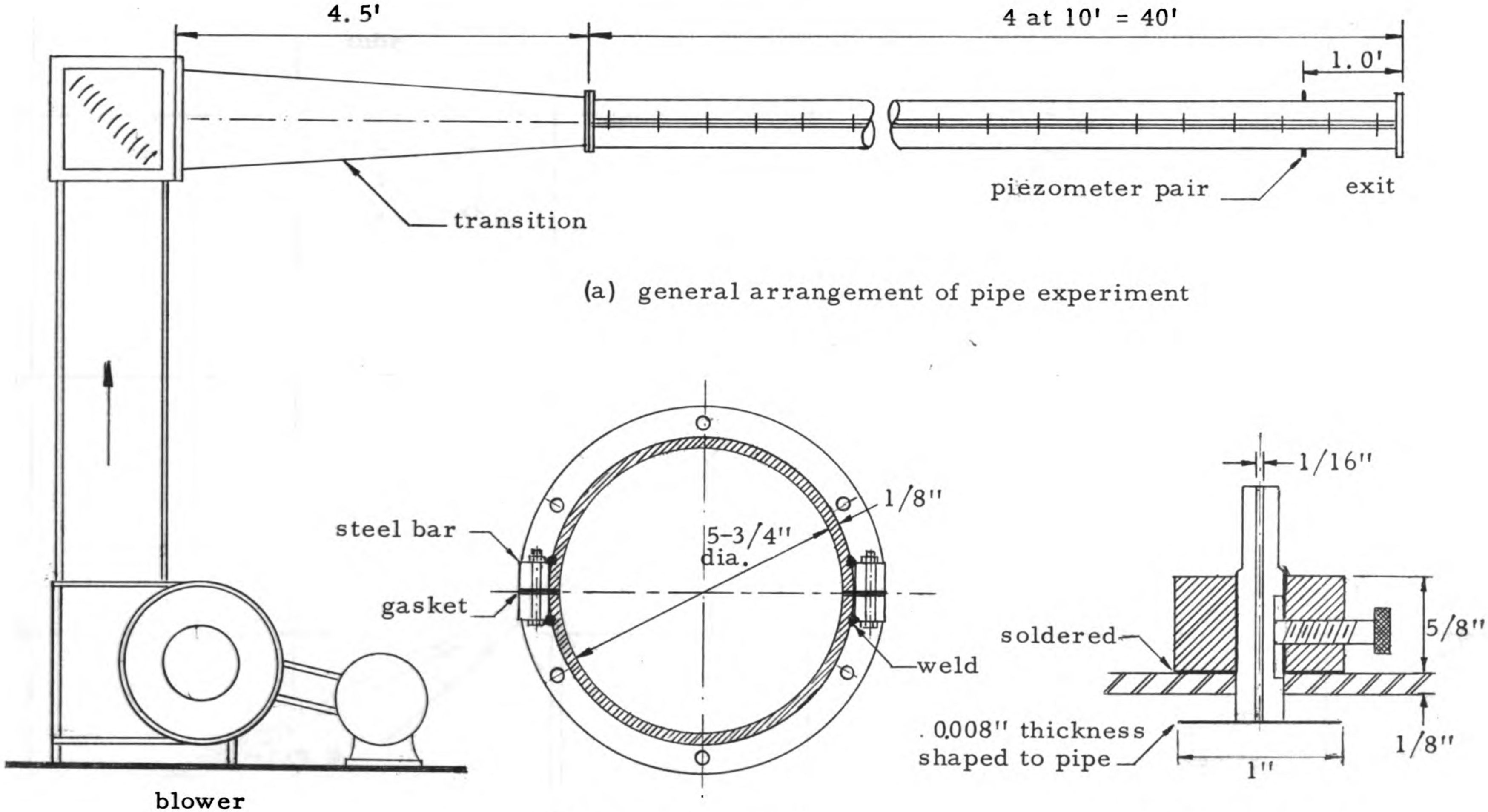

(a) general arrangement of pipe experiment

(b) pipe cross section

(c) piezometer

Figure 2. Apparatus

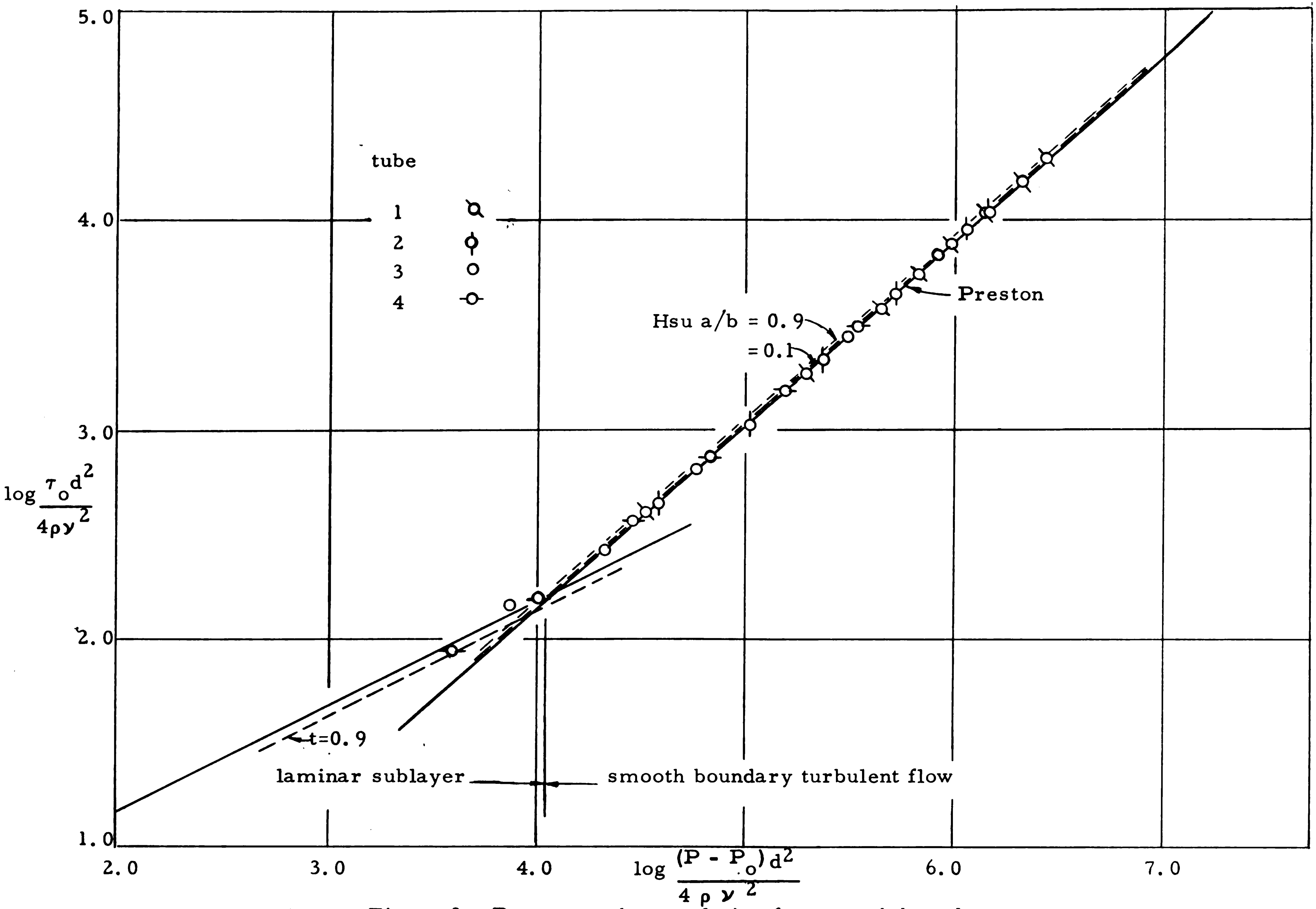

Figure 3. Pressure-shear relation for smooth boundary

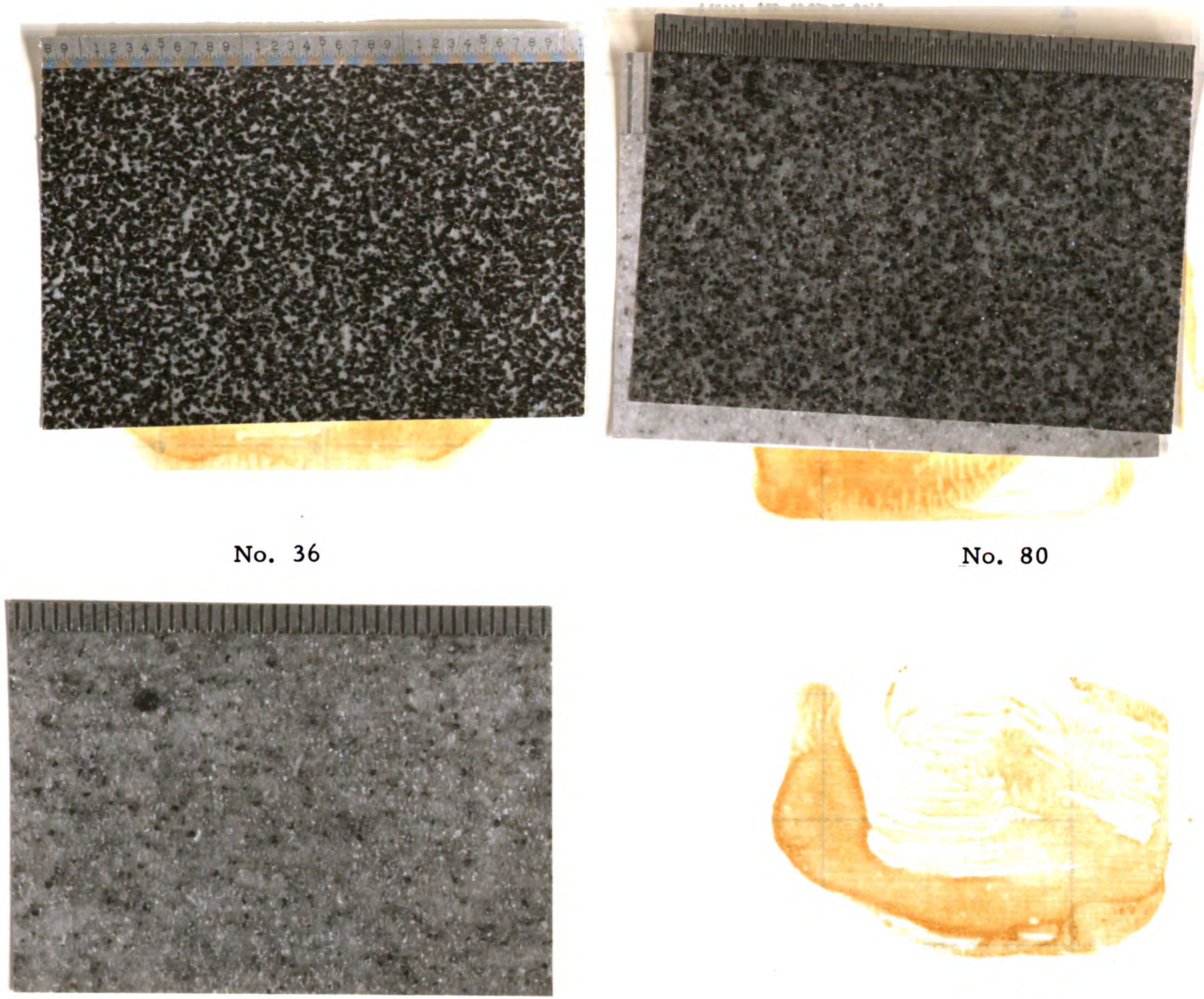

No. 36

No. 80

No. 150

No. 220

Note: one division of scale equals 0.01 inch.

Figure 5. Microphotograph of sand grains

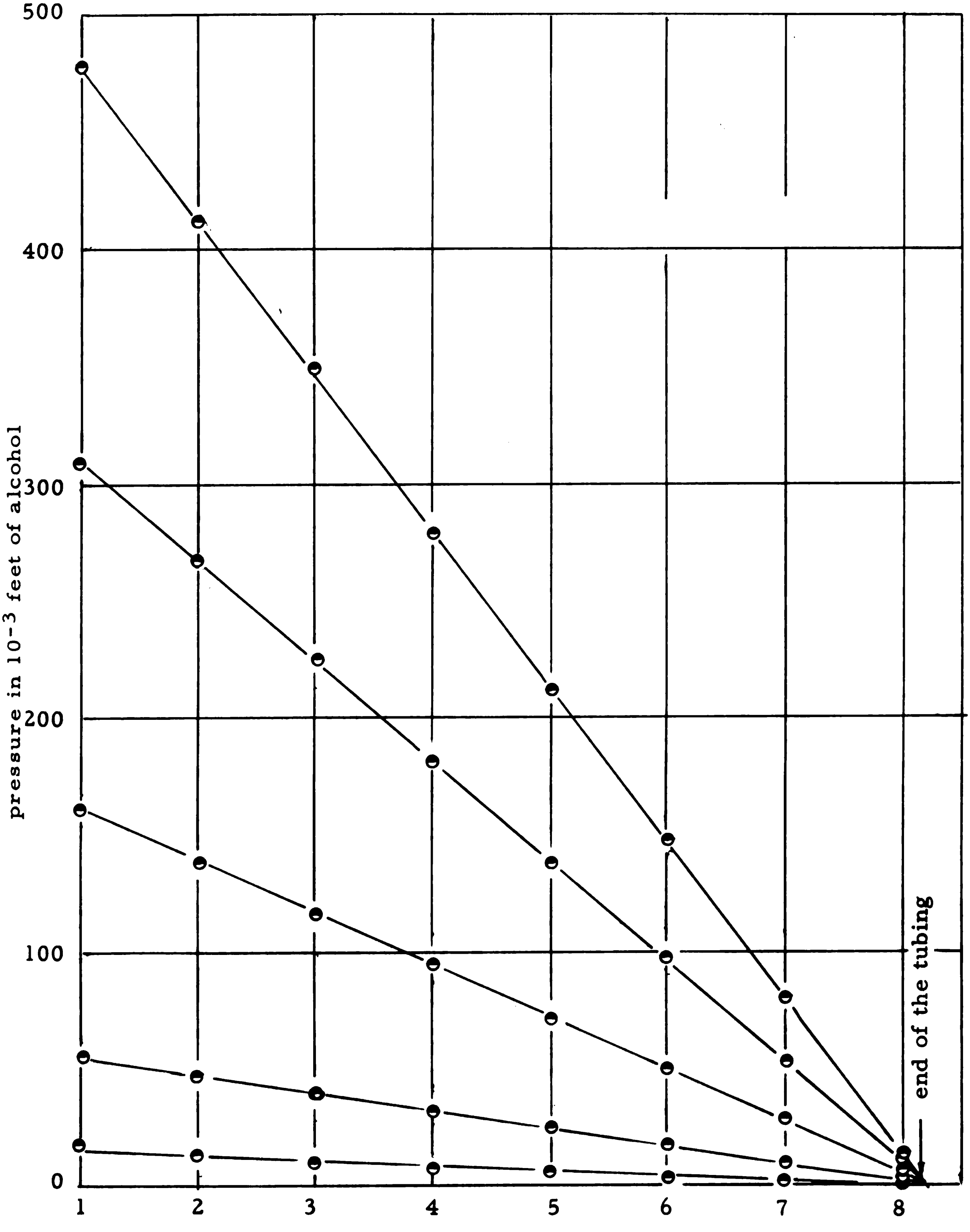

Figure 6. Typical measured pressure gradients

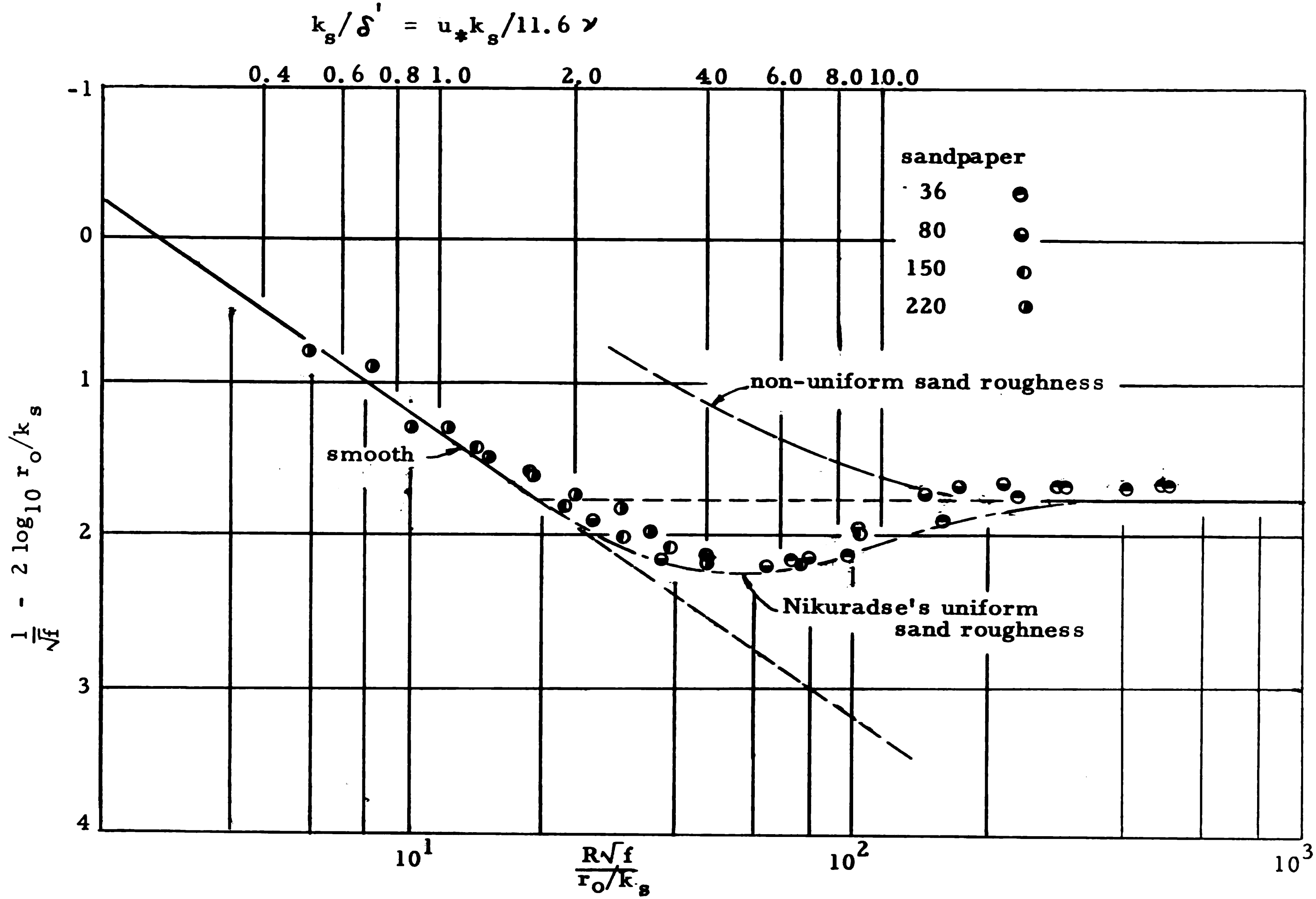

Figure 7. Resistance diagram for sandpaper roughened paper

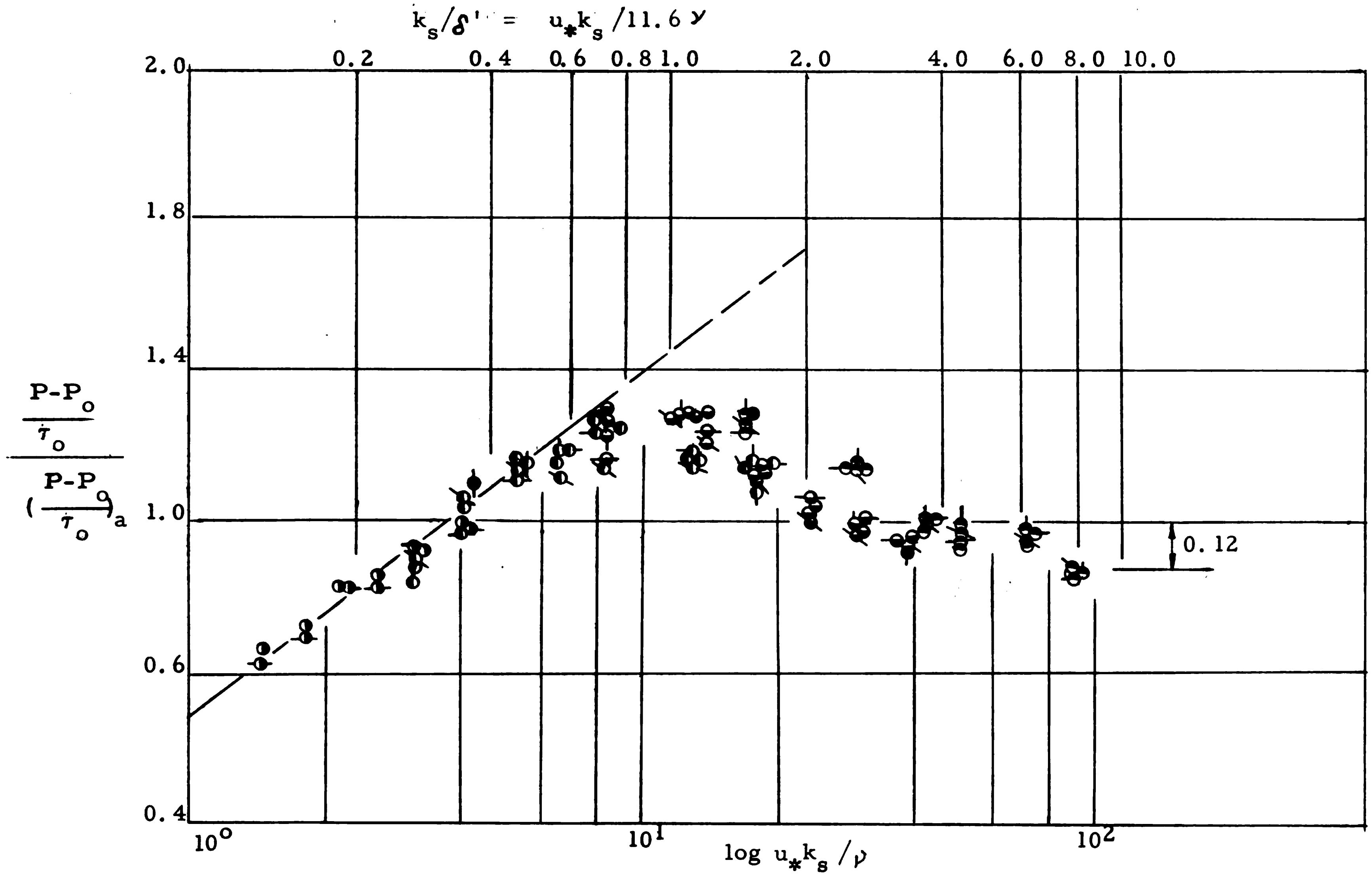

Figure 8. Correction factors for the transition regime

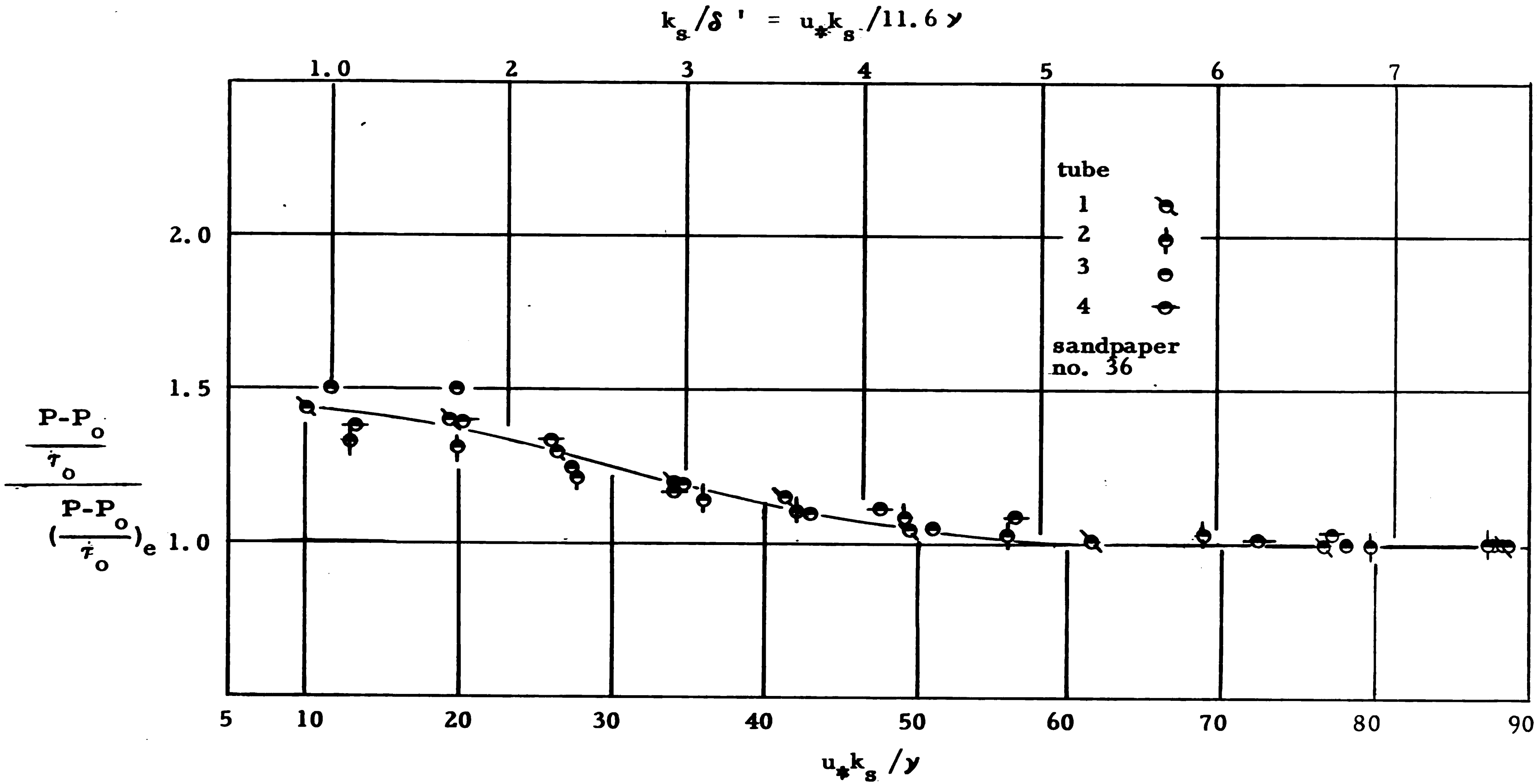

Figure 9. Effect of flow regime on pressure-shear ratio

BIBLIOGRAPHY

1. SMITH, D. W., and WALKER, J. H., "Skin-Friction Measurement in Incompressible Flow," NACA Technical Note 4231, 1958.

2. ABARBANEL, S. S., HAKKINEN, R. J., and TRILLING, L., "Use of a Stanton Tube for Skin-Friction Measurements," NASA Memorandum 2-17-59W, 1959.

3. LUDWEIG, H., "Instrument for Measuring the Wall Shearing Stress of Turbulent Boundary Layer," NACA Technical Memorandum 1284, 1950.

4. PRESTON, J. H., "The Determination of Turbulent Skin Friction by Means of Pitot Tubes," Journal of the Royal Aeronautical Society, Vol. 54, February, 1954.

5. HSU, E. Y., "The Measurement of Local Skin Friction by Means of Surface Pitot Tubes," David W. Taylor Model Basin Research and Development Report No. 957, August, 1955.

6. NIKURADSE, J., "Laws of Flow in Rough Pipes," translated as NACA Technical Memorandum 1292, 1950.

7. WHITTAKER, E. T., and WATSON, G. N., A Course of Modern Analysis, Cambridge, New York, 1927.

8. DIXON, W. J., and MASSEY, F. J., Introduction to Statistical Analysis, McGraw-Hill Book Company, New York, 1957.

9. ROBERTSON, J. M., "The Turbulent Velocity Distribution in Rough Pipe," Proceedings of the Fifth Midwestern Conference on Fluid Mechanics.